Structure, DNA Minor Groove Binding, and Base Pair Specificity of Alkyl- and Aryl-Linked Bis(amidinobenzimidazoles) and Bis(amidinoindoles)

Terri A. Fairley,† Richard R. Tidwell, Isaac Donkor, Noreen A. Naiman, Kwasi A. Ohemeng, Richard J. Lombardy, James A. Bentley,† and Michael Cory*,†

Division of Organic Chemistry, Burroughs Wellcome Co., Research Triangle Park, North Carolina 27709, and Division of Biological Chemistry and Cell Biology, Department of Pathology, School of Medicine, University of North Carolina, Chapel Hill, North Carolina 27599

Received January 14, 1993

A series of bis(amidinobenzimidazoles) and bis(amidinoindoles) with varied linking chains connecting the aromatic groups and various modifications to the basic amidino groups have been prepared. The calf thymus (CT) DNA and nucleic acid homopolymer [poly(dA)·poly(dT), poly(dA-dT)·poly(dA-dT), and poly(dG-dC)·poly(dG-dC)] binding properties of these compounds have been studied by thermal denaturation (ΔT_m) and viscosity. The compounds show a greater affinity for poly(dA)·poly(dT) and poly(dA-dT)·poly(dA-dT) than for poly(dG-dC)·poly(dG-dC). Viscometric titrations indicate that the compounds do not bind by intercalation. Molecular modeling studies and the biophysical data suggest that the molecules bind to the minor groove of CT DNA and homopolymers. Analysis of the shape of the molecules is consistent with this mode of nucleic acid binding. Compounds with an even number of methylenes connecting the benzimidazole rings have a higher affinity for DNA than those with an odd number of methylenes. Molecular modeling calculations that determine the radius of curvature of four defined groups in the molecule show that the shape of the molecule, as a function of chain length, affects the strength of nucleic acid binding. Electronic effects from cationic substituents as well as hydrogen bonding from the imidazole nitrogens also contribute to the nucleic acid affinity. The bis(amidinoindoles) show no structurally associated differential in nucleic acid base pair specificity or affinity.

Nucleic acids are important chemotherapeutic targets in the treatment of diseases and neoplasms. Interference with gene function and prevention of transcription and translation can kill invading micro-organisms or tumor cells. Unfortunately, specificity of treatment is a problem since healthy host cells are also destroyed by nonspecific therapy. Development of sequence-selective DNA binding compounds could provide highly specific antitumor drugs, since the gene sequence of various oncogenes are known. If these sequences were specifically targeted, the healthy host cells could be spared. The current studies are directed at understanding the base pair binding specificity of DNA minor groove binding compounds.

Drugs may bind to nucleic acids by either covalent[1] or noncovalent mechanisms. Additionally, compounds may bind by stacking between the bases as does ethidium bromide (1) in a process termed intercalation,[2] or by binding to one of the grooves,[3,4] or by a combination of these two mechanisms. Since the grooves contain base sequence recognition elements, it is groove binding which provides the optimal opportunity to enhance the affinity of a sequence specific drug to a desired sequence of nucleic acids.

X-ray crystal structures of a series of minor groove binding amidino-substituted compounds, bound to the AT-rich region of a double-stranded dodecanucleotide have been determined.[5-9] These compounds 4′,6-diamidino-2-phenylindole (DAPI, 2), netropsin (4), Berenil (5), Hoechst 33258 (6), and pentamidine (7), bind in the minor groove and show higher affinity for AT-rich regions over GC base pairs because binding to the latter is sterically hindered by the presence of the bulky 2-amino group of the guanine residue that protrudes into the minor groove.[5-10] The binding of compounds to the minor groove of nucleic acids is also affected by the shape of the molecule. Molecules having the optimal shape and spacing of functional groups will bind optimally to the minor groove.[11,12] Goodsell and Dickerson[12] suggest that spacing positively charged groups 5.0 Å apart provides the proper chain-repeat length while our previous work[11,13] suggests that a radius of curvature of 19 Å for the molecule is also optimal.

Crystal structures[5] suggest that the indole nitrogen on 2 forms a bifurcated hydrogen bond to two O2s of thymine on opposite strands of the DNA. There are van der Waals contacts with the floor of the groove and a general specificity for AT due to the narrowness of the groove which increases the van der Waals interaction with the aromatic systems. Compound 2 in this binding mode covers three base pairs and does not significantly alter the helical structure of the DNA.

Interaction between the amide groups of 4 and the DNA bases is also seen in crystal structures.[6] Additionally, the N1 and N5 amides of 4 form bifurcated hydrogen bonds between the adenine N3 and the thymine O2 of consecutive base pairs on opposite strands.[14] The N-methylpyrrole rings fit well into the minor groove, parallel to the groove walls. The DNA helix is not markedly affected by compound binding. The minor groove is widened slightly, and the helix axis is bent back, away from the drug, by only about 8°.

Electrostatic calculations on nucleic acids suggest that the minor groove in AT-rich segments of nucleic acids have the highest negative electrostatic potential. It is not surprising that highly cationic molecules might show AT specificity irrespective of their hydrogen bonding capabilities.[15]

The minor groove in AT-rich segments of nucleic acids

† Burroughs Wellcome Co.

0022-2623/93/1836-1746$04.00/0

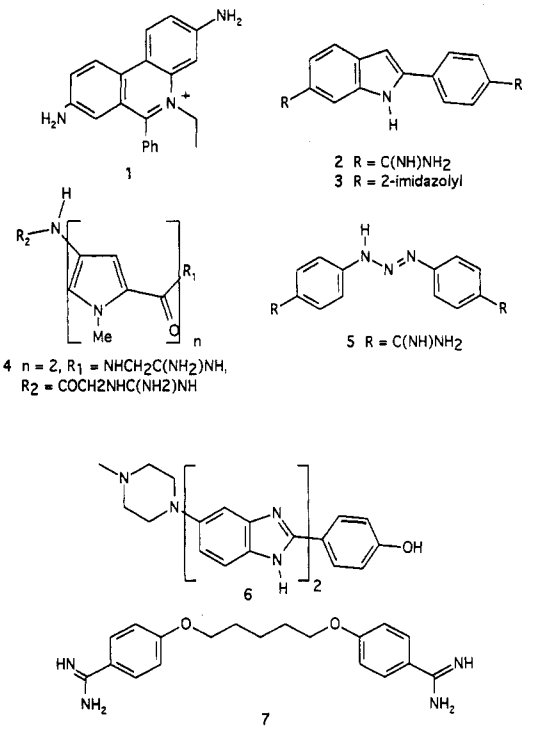

Figure 1. DNA binding molecules.

Scheme I

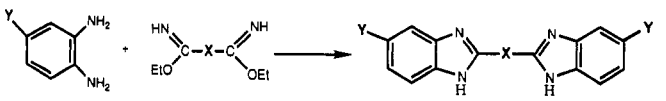

Cmpd #	Y	X
13	-H	$-(CH_2)_2-$
14	$-NO_2$	$-(CH_2)_2-$
21	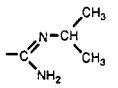	$-(CH_2)_2-$
23	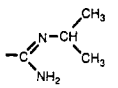	
27	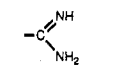	$-(CH_2)_4-$
32	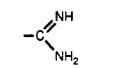	
42	-CN	$-CH_2-$
43	-CN	$-(CH_2)_4-$

is narrower than the minor groove in GC-rich sections. This narrow groove allows for optimal hydrophobic interaction between the drug and the walls of the groove. Hydrogen bonding with the bases on the floor of the groove appears to aid in drug positioning and contribute significantly to affinity. In compound **4** base pair specificity is conferred by van der Waals contacts between the adenine C2 hydrogen and the pyrrole 3-CH.[16] This close contact could not occur if the base was guanine and had an amino group at C2. The melting temperature of a complex between DNA and an analogue of **4** increased with the addition of methylpyrrole groups.[16] Correspondingly, the T_m temperature of a complex between DNA and an analogue of **4** decreased when the number of basic groups on the analogue was decreased.[16,17]

The crystal structure[9] of the polynucleotide complex with **7** indicates that the basic nitrogen atoms on the amidino group interact with the floor of the minor groove. Similarly, in **4**, the charged amidino and guanidino groups are not associated with the phosphate backbone but are centered in the bottom of the minor groove.[6]

In previous studies, we examined the DNA binding activity[11] of a series of antimicrobial bisbenzamidines[18,19] related to **7**, which is used clinically to treat *Pneumocystis carinii* pneumonia. That work showed that the DNA affinity of **7** and its analogs, as measured by a thermal denaturation assay, could be correlated with the shape of the molecular mechanics models of the compounds. The molecules which most closely fit the curvature of the minor groove had the highest polynucleotide affinity. In the series of compounds related to **7**, structures with an odd number of atoms connecting the benzamidine moieties were shown to have substantial curvature and high DNA affinity, while those with an even number of atoms connecting the benzamidines had a substantially lower affinity. The molecular modeling results showed that compounds with an odd number of atoms connecting the benzamidines had a radius of curvature closely approximating that of the nucleic acid minor groove while those with an even number of atoms were essentially linear.[11] The recent crystal structure of **7** bound to an oligonucleotide[9] confirms this model and the molecular mechanics that led to it.[20]

This paper continues the study of minor groove binding molecules and examines a series of bis(amidinobenzimidazoles) and bis(amidinoindoles). These compounds have the appropriate steric and electrostatic properties to show high-affinity binding to the minor groove of DNA. On the basis of our previous work[11] and compounds such as **2** and **6**, this new series of curved, flexible, but predominantly planar molecules were predicted to have a high affinity for the minor groove of DNA.[12]

Chemistry

The synthesis of compounds **8**, **11**, **12**, **22**, **25**, **29–31**, **33**, and **39**[21] have been reported. Compounds **19**, **20**, **26**, and **34** were a gift of H. Lowe of Hoechst AG, Frankfurt, Germany. Compounds **13**, **14**, **21**, **23**, **27**, and **32** were synthesized by reacting the appropriate substituted *o*-phenylenediamines with the appropriate diimidates as shown in Scheme I. Compound **15** was prepared by reduction of the corresponding dinitro derivative **14**. Compounds **16** and **17** were obtained by reacting the diamine **15** with either 2-chloroethyl ether to give compound **16** or 2-bromoethanol for the synthesis of compound **17**. The bis[5-cyano-(2-imidazolinyl)-2-benzimidazolyl)] derivatives **9** and **28** were prepared from 1,2-bis(5-cyano-2-benzimidazolyl)methane (**42**) and 1,4-bis(5-cyano-2-benzimidazolyl)butane (**43**), respectively. Both starting dinitriles were prepared according to Scheme I and converted to the corresponding bisimidates using standard Pinner conditions,[22] and the imidates were reacted with ethylenediamine to give the desired products. The aminomethyl derivative **18** was prepared from the corresponding dinitrile **42** by reduction over PtO_2.

Compound **24** was synthesized by reacting 3,4-diamino-*N*-isopropylbenzamidine with 2,3-dimethylmaleic anhydride in polyphosphoric acid (Scheme II). The reaction

Scheme II

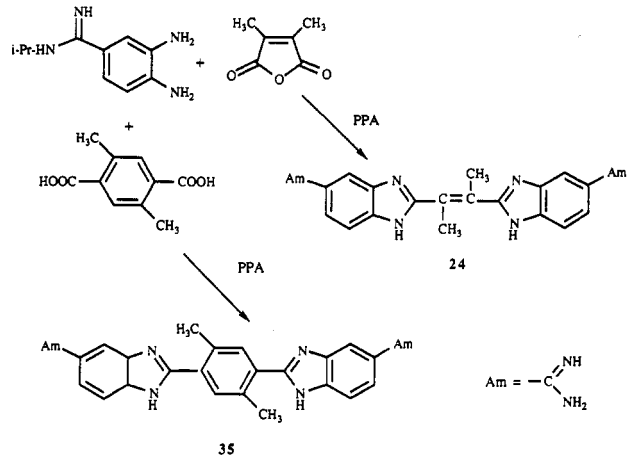

Scheme III

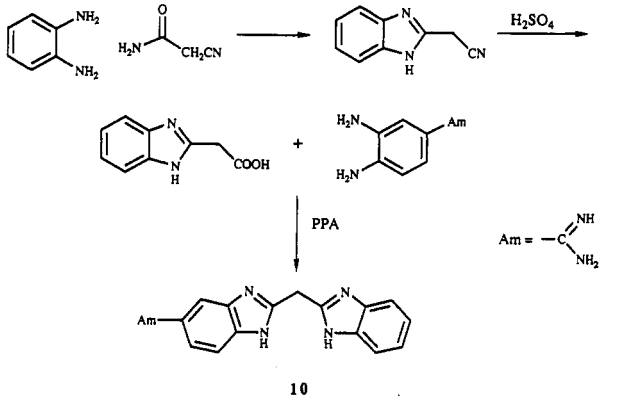

Scheme IV

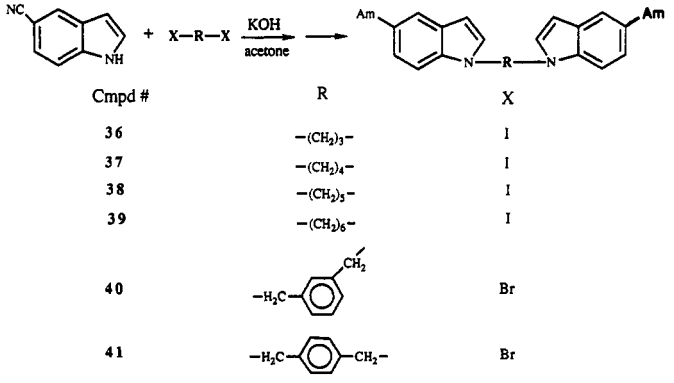

Cmpd #	R	X
36	$-(CH_2)_3-$	I
37	$-(CH_2)_4-$	I
38	$-(CH_2)_5-$	I
39	$-(CH_2)_6-$	I
40		Br
41		Br

conditions resulted in the cleavage of the isopropyl groups to give the unsubstituted amidines. Likewise, 1,4-bis(5-amidino-2-benzimidazolyl)-2,5-dimethylbenzene (**35**) was synthesized by reacting 3,4-diamino-*N*-isopropylbenzamidine with 2,5-dimethylphthalic acid.

The lone asymmetric monoamidino compound in this series, (5-amidino-2-benzimidazolyl)(2-benzimidazolyl)-methane (**10**) was prepared according to the method shown in Scheme III. This synthesis involved the reaction of 2-cyanoacetamide with *o*-phenylenidiamine to give 2-(cyanomethyl)benzimidazole.[23] The nitrile group was hydrolyzed to the acid and condensed with 3,4-diaminobenzamidine in polyphosphoric acid to give the product.

The bisindoles **36–38**, **40**, and **41** were prepared from the corresponding dinitriles in the usual manner.[21,22] The dinitriles were synthesized according to Scheme IV by the addition of 2 mol of 5-cyanoindole to the appropriate diiodoalkane or α,α-dibromoxylene in the presence of KOH and acetone. This reaction has been described in detail for the synthesis of Compound **39**[21] and was carried out in an identical manner for the novel compounds reported here. The physical properties of all of the novel compounds are reported in Table III.

Results and Discussion

Linking Groups. The results of thermal denaturation and viscosity experiments on the bis(amidinobenzimidazoles) and bis(amidinoindoles) are reported in Tables I and II. The data in Table I indicate that the compounds containing linkers with an even number of carbon atoms have a higher affinity for CT DNA and the homopolymer poly(dA)·poly(dT) than the linkers with and odd number of carbons. The type of charged substituent, amidine, imidazoline, or other substituted amidine, is not a consistent factor in increasing the poly(dA)·poly(dT) affinity. In our previous study of analogues[11] of **7**, linkers with an odd number of atoms showed a higher affinity than linkers with an even number of atoms. In the previous series, the differences between the odd and even number of atoms was considerably attenuated as the chain length increased. This attenuation with length suggests that it requires less energy, overall, to perturb any of the longer compounds, which have more torsional degrees of freedom, into an effective binding shape. This same effect of length is seen in the bis(amidinobenzimidazole) series. With the longer chain lengths, one end of the molecule might also be expected to have less dependence upon the binding of the other end because it has more rotational freedom. The data for the poly(dG-dC)·poly(dG-d) ΔT_ms in these series show the same pattern, but the results are not as clear because of the small magnitude of the ΔT_ms for poly(dG-dC)·poly(dG-dC) and the experimental error in the assay. The ΔT_ms for the bis(amidinoindoles) show no correlation with chain length for any of the polymers.

The radius of curvature data in Table I indicates that there is an optimal radius of curvature for strong poly(dA)·poly(dT) binding of the methylene-linked bisbenzimidazoles. Compounds with a radius of curvature of around 20 Å have the highest ΔT_m. This corresponds well with the 19 Å radius of curvature of the minor groove of poly(dA)·poly(dT). The radius of curvature in Table II for all four methylene-linked bisindoles is the same irrespective of the chain length. These compounds cannot assume the proper shape necessary to achieve a high-affinity complex with the DNA. The compounds have similar low DNA affinity due to electrostatic interactions with the DNA groove, but no shape contribution that could promote high DNA affinity.

Comparison of the unsaturated linkers in compounds **22** and **23** indicates that in this case the *N*-isopropylamidino group decreases AT affinity. This pattern is not seen consistently throughout the bisbenzimidazole series. In the aromatic series, comparing **33** to **34**, the isopropyl group affords increased AT and GC binding. More work is needed to fully understand the influence of bulky substituents on the amidine group.

The homopolymer binding properties of the aromatic linked bisbenzimidazoles are more complicated. There appears to be no relationship between the radius of curvature and the ΔT_ms for AT homopolymer among the compounds linked by aromatic groups. Compound **32**, the *meta*-compound, has a higher ΔT_m than the related compound with a three-methylene linker, **25**, although

Table I: Nucleic Acid Binding and Radius of Curvature of Bis(amidinobenzimidazoles)

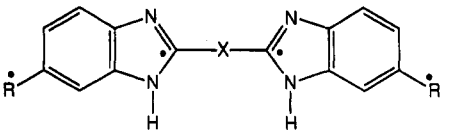

no.	R	X	radius of curvature, Å	ΔT_m, °C CT[a]	AT[b]	alternating AT	alternating GC	AT/GC ratio	viscosity slope: CT
1, ethidium bromide				12.4 (0.6)	9.9 (1.3)	16.8 (1.0)	5.3 (0.7)	3	1.1
2, DAPI			530[c]	21.5 (0.8)	38.8 (2.5)	40.5 (0.5)[f]	6.9 (0.7)	6	0.4
3, DIPI				22.4 (1.4)	45.3 (2.4)	42.7 (1.4)	9.4 (0.4)	5	0.7
4, netropsin			15	19.0 (1.8)	46.6 (0.1)	35.1 (3.8)[f]	1.1 (0.0)	32	
6, Hoechst 33258				14.1 (1.1)	32.4 (0.4)	24.1 (0.8)	2.5 (0.3)	10	
7, Pentamidine			18	10.7 (0.6)	22.9 (0.7)	20.2 (0.3)	3.2 (0.5)	6	0.2
8	amidine	$-CH_2-$	120[d]	7.6 (1.3)	9.2 (0.5)	11.5 (0.3)	3.5 (0.2)	3	0.1[g]
9	imidazoline	$-CH_2-$		6.9 (0.6)	13.5 (1.1)	10.7 (0.3)	4.1 (0.5)	3	
10	monoamidine	$-CH_2-$		1.4 (0.4)	1.3 (0.7)	1.0 (0.2)	0.2 (0.2)		
11	amidine	$-(CH_2)_2-$	23	18.5 (1.5)	42.4 (0.7)	37.2 (1.3)	4.0 (0.5)	4	
12	imidazoline	$-(CH_2)_2-$		18.5 (0.2)	40.0 (0.9)	34.6 (1.7)[f,h]	3.0 (0.5)	12	
13	H	$-(CH_2)_2-$		4.3 (0.5)	2.1 (0.3)	0.1 (0.0)	1.0 (0.2)		
14	nitro	$-(CH_2)_2-$		1.5 (0.1)	0.5 (0.3)	0.2 (0.1)	2.6 (0.1)		
15	amine	$-(CH_2)_2-$		1.6 (1.1)	3.0 (0.1)	0.6 (0.2)	2.6 (0.0)		
16	morpholine	$-(CH_2)_2-$		0.6 (0.5)	0.9 (0.0)	0.8 (0.0)	−0.3 (0.1)		
17	iminoethanol	$-(CH_2)_2-$		2.0 (0.2)	4.5 (0.1)	1.4 (0.2)	0.7 (0.4)	3	
18	aminomethyl	$-(CH_2)_2-$		12.8 (0.7)	34.2 (0.3)	14.1 (4.4)[e,h]	3.9 (0.2)	4	
19	1,4,5,6-tetrahydro-2-pyrimidine	$-(CH_2)_2-$		19.7 (0.3)	45.1 (1.3)	39.5 (0.8)[e]	2.7 (0.4)	15	
20	1,4,5,6-tetrahydro-1-methylpyrimidine	$-(CH_2)_2-$		13.3 (0.3)	30.7 (1.9)	28.9 (0.8)	1.6 (0.2)	18	
21	*N*-isopropylamidine	$-(CH_2)_2-$		19.2 (0.4)	37.3 (0.2)	32.9 (1.3)	3.3 (0.4)	10	
22	amidine	−CH=CH− (trans)	22	21.8 (0.0)	46.1 (1.3)	42.4 (0.6)[e]	5.8 (0.2)	7	−0.3[g]
23	*N*-isopropylamidine	−CH=CH− (trans)		22.8 (0.6)	31.6 (0.4)	22.5 (3.2)[e,h]	5.5 (0.4)	5	
24	amidine	$-C(CH_3)=C(CH_3)-$ (trans)		14.1 (0.3)	17.3 (1.1)	15.6 (0.7)	4.6 (0.3)	3	
25	amidine	$-(CH_2)_3-$	67	10.6 (0.5)	30.6 (0.1)	20.1 (1.0)	3.3 (0.3)	6	0.1[g]
26	imidazoline	$-(CH_2)_3-$		9.9 (0.2)	24.8 (2.5)	20.1 (0.3)	3.4 (0.9)	6	
27	amidine	$-(CH_2)_4-$	39	15.9 (0.5)	33.5 (0.2)	31.3 (0.4)	3.3 (0.5)	9	
28	imidazoline	$-(CH_2)_4-$		15.3 (0.2)	34.5 (0.3)	28.9 (0.0)	4.6 (0.1)	6	
29	amidine	$-(CH_2)_5-$	11	10.1 (0.2)	24.7 (0.1)	18.3 (0.6)[e]	3.8 (0.4)	5	
30	amidine	$-(CH_2)_6-$	28	13.5 (0.0)	34.0 (0.6)	28.0 (0.3)	3.5 (0.8)	8	
31	amidine	$-(CH_2)_8-$	32	10.2 (0.0)	22.8 (0.4)	21.2 (0.4)	3.2 (0.0)	7	
32	amidine	1,3-phenylene	10	12.9 (1.4)	34.6 (0.4)	23.9[e,g]	5.6 (0.4)	4	
33	amidine	1,4-phenylene		13.5 (0.8)	27.5 (0.1)	21.7 (2.2)[e]	3.1 (0.8)	7	
34	*N*-isopropylamidine	1,4-phenylene	23	22.3 (0.1)	44.3 (0.7)	45.0 (0.4)	5.6 (0.4)	8	
35	amidine	2,5-dimethyl-1,4-phenylene		15.6 (0.5)	29.0 (1.2)	26.5 (1.7)	3.7 (0.2)	7	

[a] CT is sonicated calf thymus DNA. [b] AT is sonicated poly(dA)·poly(dT) homopolymer. [c] From a molecular model. Crystal structure bound to DNA shows water mediated minor groove binding (ref 5). [d] From an X-ray crystal structure; molecular model is 42.1 Å. [e] Biphasic. ΔT_m determined in the same manner as for monophasic compounds. [f] Not consistently biphasic. [g] One determination only. [h] High standard deviation due to biphasic nature.

Table II: Nucleic Acid Binding of Bis(amidinoindoles)

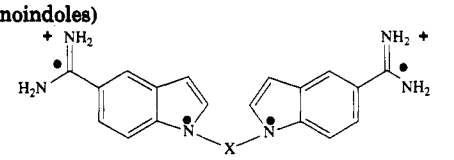

no.	X	radius of curvature, Å	ΔT_m, °C[b] CT	AT	alternating AT	alternating GC	AT/GC ratio	viscosity slope: CT
36	$-(CH_2)_3-$	14	13.7 (0.3)	19.2 (1.0)	20.3 (0.8)	6.5 (0.2)	3.1	0.1[c]
37	$-(CH_2)_4-$	9	12.1 (0.3)	18.2 (0.5)	16.3 (1.6)[d]	7.3 (0.6)	2.2	
38	$-(CH_2)_5-$	15	10.2 (0.0)	15.3 (0.8)	12.9 (1.3)	5.0 (0.0)	2.6	
39	$-(CH_2)_6-$	10	10.5 (0.8)	17.7 (0.6)	13.4 (2.3)	5.9 (0.1)	2.3	
40	1,3-phenylenedimethylene	20	8.1 (0.5)	8.1 (0.3)	9.2 (1.6)	4.0 (0.1)	2.3	
41	1,4-phenylenedimethylene	9	9.3 (0.8)	10.8 (0.0)	11.9 (0.4)	5.4 (0.6)	2.2	

[a,b] See corresponding footnotes of Table I. [c] See footnote *g* of Table I. [d] See footnote *f* of Table I.

the radius of curvature is shorter than optimal. It is possible that the bulky aromatic group of **32** provides added DNA affinity in comparison to the methylenes of **25**.

For the aromatic compounds, other structural factors may be influencing the nucleic acid binding in addition to the radius of curvature. For example, an optimal distance of 5.0 Å between charged groups[12] has been suggested as an important structural factor for DNA minor groove binding. The distance between the imidazole nitrogen atoms is 5.3 Å in compound **32**, close to the suggested optimum. Compounds **33** and **35** linked in the *para*-position have equal ΔT_ms, suggesting that the methyl

Table III. Physical Properties of Novel Compounds

compd	mp, °C	% yield	recryst solv	formula	analysis
13	>300	63	EtOH	$C_{16}H_{14}N_4 \cdot 2HCl$	C,H,N
21	>300	28	1 N HCl	$C_{24}H_{30}N_8 \cdot 4HCl \cdot 1H_2O$	C,H,N
23	292	7	1 N HCl	$C_{24}H_{28}N_8 \cdot 4HCl \cdot 4H_2O$	C,H,N
27	>300	5	EtOH/H_2O, 2:1	$C_{20}H_{22}N_8 \cdot 4HCl \cdot 2H_2O$	C,H,N
32	>300	20	1 N HCl	$C_{22}H_{18}N_8 \cdot 4HCl \cdot 4.4H_2O$	C,H,N
36	265	19	EtOH	$C_{21}H_{22}N_6 \cdot 2HCl \cdot 1.06H_2O$	C,H,N
37	273	34	EtOH	$C_{26}H_{24}N_6 \cdot 2HCl \cdot 0.8H_2O$	C,H,N
38	298	36	EtOH	$C_{26}H_{24}N_6 \cdot 2HCl \cdot 1.2H_2O$	C,H,N
40	265	22	HCl (10%)	$C_{23}H_{26}N_6 \cdot 2HCl \cdot 2H_2O$	C,H,N
41	262	23	EtOH	$C_{24}H_{28}N_6 \cdot 2HCl \cdot 2.75H_2O$	C,H,N

groups on the aromatic ring system do not contact the floor of the minor groove. The explanation for the enhanced affinity of compound 34 is not clear.

Viscosity. The results of viscometric titrations[11,24] using calf thymus DNA and selected compounds are shown in Table I. DAPI (2) and compound 6 gave no change in viscosity slope, indicating that the complexes between the drugs and DNA show no increase in helix chain length. This result is consistent for a minor groove binding mechanism. In a similar manner, pentamidine (7) and compounds 8, 22, 25, and 36 also showed no change in calf thymus DNA viscosity, indicating a nonintercalating mode of binding and no increase in the DNA length. Intercalating molecules such as ethidium bromide (1) show viscometric titration slopes approximating unity. Compounds 2 and, by analogy, 3 bind to AT base pairs in the minor groove but may intercalate into GC base pairs. Given the 50/50 ratio of AT to GC base pairs in calf thymus DNA, slopes between 1 and 0 might reasonably be expected for these compounds. While these experiments alone do not prove a minor groove binding mechanism, by analogy with other similar compounds (4, 5, and 7) for which polynucleotide-bound crystal structures have been reported, we conclude that these compounds bind in the minor groove.[4,6,7,9]

Side Chains. Comparison of compounds 11 with 12, 25 with 26, and 27 with 28, shows that substituting an imidazoline for an amidine has little effect on the DNA affinity. Substituting a bulky *N*-isopropyl group gives mixed results as discussed above. The six-membered ring analogue 19 of the imidazoline 12 shows the same DNA affinity, while methylation of this ring system (20) decreases affinity. These results are consistent with previous work.[11] The series of nonbasic analogs of 11, compounds 13–17, show little or no DNA affinity. The aminomethyl compound 18 is probably protonated at neutral pH, and therefore has two charges when bound to DNA, still shows substantially reduced DNA affinity in comparison to 11. The biphasic ΔT_m curve gives a high standard deviation for compound 18. This compound also shows the greatest difference between the poly(dA)·poly(dT) and the poly(dA-dT)·poly(dA-dT) results.

The monoamidine 10 has a considerably lower DNA affinity than either 8 or 9, which are bisamidines. This result indicates that the presence of a charged group on both ends of these compounds is important for positioning the compound in the groove to maximize van der Waals interactions.

Base Pair Specificity. There is an extremely high correlation between the ΔT_ms for the poly(dA)·poly(dT) and the poly(dA-dT)·poly(dA-dT) homopolymers for the bis(amidinobenzimidazoles). The major outlier for this correlation is compound 18, which shows a much lower than expected affinity for poly(dA-dT)·poly(dA-dT). Omitting compound 18 results in an r^2 of 0.96 for the remaining compounds. The elevated poly(dA-dT)·poly(dA-dT) ΔT_m for 1 is as expected. Compound 1 binds to DNA by an intercalation mechanism unlike all of the other compounds in Tables I and II, which we suggest bind in the minor groove. The higher affinity for alternating AT homopolymer could be due to an increased area of overlap between the intercalating compound and the aromatic rings of the intercalation site that would occur only on the alternating polymer.

The AT/GC ΔT_m ratios in Table I indicate that the bisbenzimidazoles show a strong AT specificity over alternating GC sites. Although the affinity of some of the bis(amidinobenzimidazoles) approaches that of 4 for the AT homopolymers, none of the compounds are as AT specific as 4. In the bis(amidinobenzimidazole) case, the lower specificity is due to higher GC binding when compared to compound 4. The higher GC affinity may occur because the bisbenzimidazoles have less bulky and more flexible methylene linkers in comparison to the amide linkers of 4. Rotations about the linking chain could allow parts of the compound to rotate into a conformation that allowed binding to GC-rich sites.

The bis(amidinoindoles) in Table II have a significantly lower affinity for DNA and the nucleic acid homopolymers than the bis(amidinobenzimidazoles) in Table I. Additionally the compounds do not show the pattern of structurally related changes in affinity seen with the compounds in Table I. The compounds in Table II also show a marked lack of base pair specificity in comparison to the bis(amidinobenzimidazoles) in Table I. This lower specificity is due to a combination of lower AT binding and higher GC binding. The DNA binding properties of the compounds in Table II resemble those of 1, an intercalator rather than a groove-binding molecule. The viscometric titration with compound 36 indicates that the smallest of these compounds does not bind by intercalation. The longer compounds would not be expected to intercalate because they would be too long to fit into an intercalation site.

The lack of base pair specificity for the bis(amidinoindoles) could be explained by the lack of additional hydrogen bond forming ligands on the bis(amidinoindoles). The lack of these extra ligands could allow only the amidino group to interact with the minor groove.

In conclusion, these studies present a series of bisamidines with a novel structural motif that still retains the properties of high DNA affinity and significant specificity for AT-rich nucleic acid homopolymers. The biophysical and molecular modeling data suggest that the compounds bind to nucleic acids in the minor groove. Increasing the bulk of the substituents on the amidine groups appears to improve the AT specificity of the compounds. Chemical modification of the correct linking chain to decrease the

flexibility of the molecule affords compounds with an extremely high affinity for AT homopolymers. Molecular modeling studies and geometric measures of the shapes of the molecules can be used within this class as tools to design molecules with high affinity.

Experimental Section

All starting materials for the synthesis were purchased from either Aldrich Chemical Co., Fisher Scientific Co., Fluka Chemical Corp., or K & K Laboratories and were used without further purification. Ammonia and hydrochloric acid were purchased from Matheson Division of Searle Medical Products. All melting points were obtained on a Thomas Hoover melting point apparatus and are uncorrected. ^{1}H-NMR spectra were obtained on either a Varian 390 90-MHz spectrometer or a Bruker 300 MHz spectrometer. Infrared spectra were obtained on a Perkin-Elmer Model 1320 spectrophotometer. Thin-layer chromatography (TLC) was performed on 100 μm thick silica gel with fluorescent indicator purchased from Eastman Kodak Comp. Column chromatography was performed using 60 mesh silica gel (Aldrich). Elemental analyses were performed by Atlantic Microlab, Norcross, GA, and are within 0.4% of the theoretical value.

4-Acetamidobenzonitrile. 4-Aminobenzonitrile (104 g, 0.88 mol) was added slowly to acetic anhydride (500 mL), and the temperature was maintained between 35 and 45 °C. After the addition was complete, the suspension was chilled on an ice bath and poured into a 1-L bath of ice/H_2O. The solid was collected by filtration and washed with H_2O until the washings were neutral. The solid was dried in the oven to afford 132 g (94%) of the desired product as a white powder, mp 203–204.5 °C (lit.[25] mp 205 °C).

4-Amino-3-nitrobenzonitrile. Potassium nitrate (52 g, 0.51 mol) was dissolved in concentrated H_2SO_4 (250 mL) and cooled to below 0 °C. 4-Acetamidobenzonitrile (40 g, 0.25 mol) was added slowly, the temperature being kept below 0 °C. The suspension was stirred at this temperature for an additional 3.5 h and then poured into 1 L of ice. The yellow precipitate was filtered and washed with a small amount of H_2O. This solid was suspended in 2 N H_2SO_4 (500 mL) and heated under reflux for 3 h. The suspension was cooled to room temperature and the solid was collected by filtration, washing with a small amount of cold H_2O to yield 35.95 g (88%) of the desired product as a bright yellow powder, mp 160–161 °C.

4-Amino-3-nitrobenzamidine. A dried sample of 4-amino-3-nitrobenzonitrile (5.0 g, 0.031 mol) was suspended in dry dioxane (75 mL) and dry MeOH (2.5 mL) and was chilled to 0–5 °C. The suspension was saturated with HCl(g), the low temperature being maintained. The flask was stoppered, and the contents were stirred at room temperature until an IR spectra indicated the disappearance of the nitrile peak. At this point, the suspension was chilled and the solid was collected by filtration under N_2 and washed with anhydrous Et_2O. The yellow solid was suspended in absolute EtOH saturated with NH_3 (125 mL), and the flask was stoppered and heated (oil bath temperature 80 °C) for 6 h. The solution was cooled on an ice bath, and the resulting precipitate was collected by filtration and washed with Et_2O to afford 5.7 g (73%) of a yellow solid as the product, mp >300 °C.

3,4-Diaminobenzamidine. A solution of 4-amino-3-nitrobenzamidine (5.69 g, 0.0225 mol) in MeOH (150 mL) and 10% Pd–C (0.57 g) was hydrogenated until the required quantity of H_2 was taken up. The solution was filtered through Celite to remove the catalyst and the MeOH was removed under reduced pressure. The resulting solid was triturated with a small amount of MeOH and collected by filtration to afford 3.97 g (95%) of the desired product, mp 237–239 °C.

3,4-Diaminobenzonitrile. A solution of 4-amino-3-nitrobenzonitrile (10 g, 0.06 mol) in EtOH (200 mL) and 0.5 g of 10% Pd–C was hydrogenated at room temperature until the required H^2 was utilized. The catalyst was removed by filtration, and the EtOH was removed under reduced pressure. The resulting solid was recrystallized from 25% EtOH to afford 7.7 g (96%) of 3,4-diaminobenzonitrile as a brown solid, mp 144–146 °C.

Bis[5-(2-imidazolinyl)-2-benzimidazolyl]methane (9). A solution of malononitrile (2.5 g, 37.8 mmol) in benzene (50 mL) and EtOH (6.2 mL) was chilled at a temperature of 5 °C in a three-neck flask fitted with a thermometer and a drying tube. The solution was saturated with HCl while the temperature was kept below 15 °C. The flask was stoppered, and the contents were stirred at room temperature until IR spectra showed that the nitrile stretch was gone. Et_2O was added, and the reaction was chilled on an ice bath. The solid was collected by filtration under N_2 and washed well with Et_2O to afford 8.4 g (96%) of the diimidate. This compound was used immediately.

This diimidate (4.4 g, 19 mmol) and 3,4-diaminobenzonitrile (5.0 g, 37.5 mmol) were suspended in glacial AcOH (15 mL) and immediately heated to reflux. After 1.5 h, the solution was cooled to room temperature and the AcOH was removed *in vacuo*. The resulting oil was suspended in H_2O (25 mL) and basified to a pH of 8 with concentrated NH_4OH. The solid was collected by filtration, suspended in EtOH, and acidified with HCl-saturated EtOH to a pH of 2. The solid was collected by filtration and washed with Et_2O to afford 4.64 g (97%) of bis(5-cyano-2-benzimidazolyl)methane, mp 310–312 °C.

Bis(5-cyano-2-benzimidazolyl)methane (2.5 g, 9.5 mmol) was suspended in benzene (150 mL) and MeOH (50 mL) in a three-neck flask as described above. The suspension was chilled on an ice bath to a temperature of 10 °C and was saturated with HCl. The flask was stoppered, and the contents were stirred at room temperature until the nitrile stretch was gone from the IR. The solution was chilled and the solid collected by filtration and washed with Et_2O. The solid was dissolved in absolute EtOH (150 mL), ethylenediamine (3.43 mL, 57 mmol) was added, and the solution was heated to reflux for 1 h. The mixture was cooled to room temperature, and the oil was stirred in H_2O. The resulting solid was collected by filtration and acidified with HCl/EtOH until pH 2. The solid was collected by filtration and dried under high vacuum to afford 2.9 g (62%) of the desired product: mp 280 °C dec; NMR (300 MHz, DMSO-d_6) 3.5 (br s, 1 H, NH benzimidazole), 3.97 (s, 8H, CH_2CH_2), 4.64 (s, 2H, CH_2), 7.78 (d of d, 4H, Ar-H), 8.32 (s, 2H, Ar-H). Anal. ($C_{21}H_{20}N_8$·2HCl·2H_2O) C, H, N.

5-Amidinobis(2-benzimidazolyl)methane (10). A mixture of 2-cyanoacetamide (33.6 g, 0.4 mol) and *o*-phenylenediamine (21.6 g, 0.2 mol) was heated to 200 °C for 45 min. The mixture melted at an oil bath temperature of 150 °C, and the progress of the reaction was monitored by following the gas evolution. The reaction was cooled, and the resulting brown solid was washed with Et_2O and then recrystallized from H_2O to afford 18.8 g (60%) of 2-(cyanomethyl)benzimidazole, mp 202–207 °C (lit.[23] mp 210–211 °C).

A solution of 2-(cyanomethyl)benzimidazole (10.0 g, 0.064 mol) in 18 N H_2SO_4 was heated under reflux for 2 h. The solution was allowed to cool to room temperature, and the precipitate was collected by filtration. The solid was dissolved in H_2O (200 mL) and filtered, and the filtrate was basified with concentrated NH_4OH. The mixture was filtered again, and the filtrate was acidified with acetic acid. The resulting solid was collected by filtration and dried to yield 8.7 g (77%) of 2-benzimidazolylacetic acid, mp 121 °C.

A solution of 2-benzimidazolylacetic acid (1.76 g, 0.01 mol) and 3,4-diaminobenzamidine (2.23 g, 0.01 mol) in polyphosphoric acid (30 g) was heated to 160 °C for 2.5 h. The hot solution was poured into H_2O (125 mL), and the solution was basified with NaOH. An oil separated from the aqueous solution, and the oil solidified upon standing. The solid was collected by filtration, dissolved in hot MeOH, and filtered and the filtrate was acidified with HCl-saturated EtOH. The filtrate volume was reduced, and the resulting solid was collected and dried to afford 480 mg (12%) of compound **10**: mp 285–295 °C; NMR (90 MHz, DMSO-d_6) 5.2 (s, 2H, CH_2), 7.45–8.0 (m, 6H, 4 unsubst Ar-H, 2 subst Ar-H), 8.25 (d, 1H, Ar-H), 9.0–9.8 (br s, 2H, NH-imidazoline). Anal. ($C_{16}H_{14}N_6$·3HCl) C, H, N.

1,2-Bis(5-nitro-2-benzimidazolyl)ethane (14). Succinonitrile (10.0 g, 0.125 mol) was dissolved by dry benzene (400 mL) and dry EtOH (21 mL). The solution was saturated with HCl gas at temperatures between 0 and 5 °C for 1.5 h. The solution was kept cold for an additional 1.5 h, and the white precipitate that formed was collected by filtration under N_2 and washed with anhydrous Et_2O to afford 30 g (98%) of the imidate hydrochloride of succinonitrile. A suspension of the imidate (25

g, 0.102 mol) and 1,2-diamino-4-nitrobenzene (31.26 g, 0.204 mol) in glacial acetic acid was heated under reflux for 10 h. The resulting solid was collected by filtration, stirred with 5% NH_4OH, filtered, and washed with H_2O until the filtrate was neutral. Recrystallization from EtOH/H_2O (2:1) acidified with concentrated HCl afforded 39 g (45%) of the desired compound: mp 290 °C dec; NMR (90 MHz, DMSO-d_6) 3.58, (s, 4H, CH_2CH_2), 7.74 (d, 2H, Ar-H), 8.12 (d, 2H, Ar-H), 8.45 (s, 2H, Ar-H). Anal. ($C_{16}H_{12}N_6O_4$) C, H, N.

1,2-Bis(5-amino-2-benzimidazolyl)ethane (15). A solution of 14 (4.0 g, 11 mmol) in 70% aqueous TFA (100 mL) was hydrogenated over 10% Pd–C (0.8 g) at 30 psi for 1 h. The catalyst was removed by filtration and washed with 70% aqueous TFA (50 mL). The solvents were removed *in vacuo*, and the residue was dissolved in H_2O and basified (pH 8) with NH_4OH. The precipitate was collected by filtration and washed with H_2O. Recrystallization from EtOH/H_2O (5:1) acidified with concentrated HCl yielded 3.75 g (90%) of 15: mp >300 °C; NMR (90 MHz, DMSO-d_6) 3.25 (s, 4H, CH_2CH_2), 5.50 (br s, 4H, NH_2), 6.50 (d, 2H, Ar-H), 6.68 (s, 2H, Ar-H), 7.22 (d, 2H, Ar-H). Anal. ($C_{16}H_{16}N_6$·2HCl) C, H, N, Cl.

1,2-Bis(5-morpholino-2-benzimidazolyl)ethane (16). Bis-(2-Chloroethyl) ether (3 mL) was added to a solution of 1,2-bis-(5-amino-2-benzimidazolyl)ethane (3.5 g, 12 mmol) and TEA (7 mL) in EtOH (50 mL). The mixture was heated under reflux for 2 weeks, cooled to room temperature, and concentrated to dryness. The residue was dissolved in H_2O and basified with NH_4OH (pH 10). The precipitate was collected by filtration and washed with H_2O until the filtrate was neutral. The solid dissolved in EtOH and acidified with concentrated HCl. The EtOH was removed under reduced pressure, and the residue was recrystallized from MeOH to afford 2.8 g (46%) of the desired product: mp 273 °C; NMR (90 MHz, DMSO-d_6) 3.4 (br s, 8H, NCH_2), 3.95 (m 12H, $ArCH_2CH_2Ar$, CH_2OCH_2), 7.5–7.9 (m 6H, Ar-H), 9.6 (br s, 6H, NH, NH^+). Anal. ($C_{24}H_{28}N_6O_2$·2.2HCl) C, H, N, Cl.

1,2-Bis[5-[(2-hydroxyethyl)amino]-2-benzimidazolyl]ethane (17). 2-Bromoethanol (1.71 g, 13.7 mmol) and TEA (2 mL) were added to a solution of 1,2-bis(5-amino-2-benzimidazolyl)ethane (2.0 g, 6.85 mmol) in EtOH (30 mL). The mixture was heated under reflux for 3 d, cooled to room temperature, and concentrated to dryness. The residue was washed with H_2O, suspended in EtOH, and acidified with concentrated HCl. The precipitate was collected by filtration and dried under vacuum to yield 2.7 g (87%) of 17: mp >300 °C; NMR (90 MHz, DMSO-d_6) 3.0–3.4 (m 10H, NCH_2CH_2OH), 3.65 (m, 4H, $ArCH_2CH_2Ar$), 5.4–6.3 (br s, 4H, NH), 6.5 (m, 4H, Ar-H), 7.2 (d, 2H, Ar-H). Anal. ($C_{20}H_{24}N_6O_2$·3.7HCl·H_2O) C, H, N. Cl.

1,2-Bis[5-(aminomethyl)-2-benzimidazolyl]ethane (18). The imidate of succinonitrile was made as described. A solution of 3,4-diaminobenzonitrile (1.7 g, 13 mmol) and the succinonitrile imidate (1.5 g, 6.5 mmol) in glacial acetic acid (25 mL) was heated under reflux for 8.5 h. The reaction was cooled to room temperature and the volume reduced to one-third. Water was added, and the mixture was basified with NH_4OH. The precipitate was collected by filtration, dissolved in MeOH, and decolorized with charcoal. The charcoal was removed by filtration and washed with aqueous acetic acid. The solvent was removed under reduced pressure, and the solid was suspended in MeOH, acidified with concentrated HCl, and hydrogenated over PtO_2 at room temperature for 6.5 h. The catalyst was removed by filtration and the solvent removed *in vacuo*. The residue was decolorized with charcoal in a mixture of EtOH/10% HCl (1:1). The charcoal was removed by filtration, and the solvents were removed under reduced pressure to afford 2.4 g (92%) of the desired product: mp >300 °C; NMR (90 MHz, DMSO-d_6) 4.3 (s, 4H, $ArCH_2CH_2Ar$), 4.73 (s, 4H, $ArCH_2N^+$), 8.00 (m, 4H, Ar-H), 8.3 (s, 2H, Ar-H). Anal. ($C_{18}H_{20}N_6$·4.1HCl) C, H, N, Cl.

***E*-3,4-Bis(5-amidino-2-benzimidazolyl)butene (24).** A mixture of dimethylmaleic anhydride (1.4 g, 11 mmol) and 3,4-diamino-*N*-isopropyl benzamidine (5.1 g, 22 mmol) in polyphosphoric acid (80 g) was heated to 90–100 °C until the foaming stopped (approximately 30 min). The solution was then gradually warmed to 200 °C and was maintained at this temperature for 1.5 h. The mixture was poured into ice/H_2O (250 mL) and filtered, and the filtrate was basified to pH 8–9. The resulting precipitate was filtered, dissolved in 2 N HCl (200 mL), and decolorized with activated charcoal while being heated at 100 °C. The charcoal was removed by filtration, and the filtrate was basified to pH 8. The resulting solid was collected by filtration, acidified with 2 N HCl, and recrystallized from H_2O to afford 500 mg (16%) of the desired product: mp >300 °C; NMR (90 MHz, TFA-*d*) 2.78 (s, 6H, CH_3), 8.14 (m, 4H, Ar-H), 8.245 (d, 2H, Ar-H). Anal. ($C_{20}H_{20}N_8$·3HCl·1.6H_2O) C, H, N.

1,4-Bis[5-(2-imidazolinyl)-2-benzimidazolyl]butane (28). This compound was synthesized as described for bis[5-(2-imidazolinyl)-2-benzimidazolyl]methane. The diimidate made from 1,4-dicyanobutane (94%) was condensed with 3,4-diaminobenzonitrile under the same conditions to afford 49% of the intermediate 1,4-bis(5-cyano-2-benzimidazolyl)butane, mp 335 °C dec. The diimidate of this compound was made and reacted with ethylenediamine to yield 60% of the desired product: mp 319–321 °C; NMR (300 MHz, DMSO-d_6) 2.05 (s, 4H, CH_2CH_2-CH_2CH_2), 3.17 (s, 4H, Ar-CH_2), 4.0 (s, 4H, imidazole-CH_2), 4.5 (br s, 2H, NH), 7.92 (d of d, 4H, Ar-H), 8.30 (s, 2H, Ar-H), 10.9 (s, 4H, NH_2^+). Anal. ($C_{24}H_{26}N_8$·3HCl) C, H, N.

1,4-Bis(5-amidino-2-benzimidazolyl)-2,5-dimethylbenzene (35). A mixture of 2,5-dimethylphthalic acid (1.7 g, 9 mmol) and 3,4-diamino-*N*-isopropylbenzamidine (4.0 g, 17 mmol) in polyphosphoric acid (150 g) was heated at 110 °C for 45 min and then gradually warmed to 200 °C for 2 h. The mixture was poured into ice/H_2O (500 mL), and the resulting solid was collected by filtration and suspended in 10% $NaHCO_3$. The solid was collected by filtration and recrystallized in aqueous EtOH/HCl (pH 2) to yield 3.0 g (59%) of the desired product: mp 294 °C; NMR (90 MHz, DMSO-d_6) 2.77 (s, 6H, CH_3), 7.93 (m, 6H, benzimidazole-H), 8.33 (s, 2H, Ar-H), 9.27 (d, 6H, Am-H). Anal. ($C_{24}H_{22}N_8$·3HCl·1.8H_2O·0.5EtOH) C, H, N.

Calf Thymus DNA and Deoxyribonucleic Acid Homopolymer Experiments. The methods used for the calf thymus DNA and homopolymer ΔT_ms, and the viscometric titrations reported in Tables I and II, are essentially those described by Cory.[26,11] A few compounds in Table I show biphasic T_m behavior. The ΔT_m for these compounds were determined in the same manner as for the other compounds. However, if the ΔT_m occurs within the flat part of the biphasic curve, larger errors in ΔT_m are seen than in the usual experiments. These biphasic results are noted in Table I. Typical T_m values for the calf thymus DNA and homopolymers under these experimental conditions are as follows: calf thymus DNA = 56.6 ± 0.8 °C, poly(dA)·poly(dT) = 40.9 ± 0.5 °C, poly(dG-C)·poly(dG-C) = 83.2 ± 1.2 °C, poly(dA-dT)·poly(dA-dT) = 36.8 ± 1.0.

Molecular Modeling. Molecular mechanics models of the compounds for which radius of curvature data appears in Tables I and II were generated as reported by Cory[11] using version 3.0 of MacroModel.[27] The molecules were minimized with the imidazole of the benzimidazole ring system unprotonated. Torsional searches of the terminal linking chain atoms followed by minimization of the connecting chain were performed to ensure that the structures were at a global minimum. A FORTRAN 77 program implementing the previously described algorithm to calculate the radius of curvature[11] was run on a DEC/VAX computer under the VMS operating system. This program operated directly upon the MacroModel structure file. The radius of curvature measurements, presented in Tables I and II, are done with four atoms. The four atoms used in the calculation are highlighted with a dot (·) in the structures heading Tables I and II. The atoms, for the radius of curvature measurement, were chosen to be insensitive to small differences in torsion angles, to bisect the molecule, and give the best representation of the overall shape of the molecule.

A preliminary series of calculations was necessary to provide parameters for molecular mechanics in the amidinobenzimidazole series. 5-Amidinio-2-methylbenzimidazole and its tautomer 6-amidinio-2-methylbenzimidazole were built in the MacroModel program and the geometry was optimized using Gaussian 88[28] with the 6-31G basis set. This basis set was chosen to give the best compromise between accuracy and computational time. The optimized geometry was then used as input for a G80/UCSF[29] calculation of potential fit charges. These calculations were done using the STO-3G basis set. These charges were then added to the AMBER force field of MacroModel as a template.

Additional computations were done on the benzimidazole

system to determine the effect of the proximity of the amidine to the imidazole NH. The amidinobenzimidazole tautomer with the amidino group closest to the NH has the highest energy (distant isomer, Hartree–Fock energy -564.63570, close isomer -564.63158, difference in relative energy 2.59 kcal), a result consistent with increased energy due to through-space charge repulsion between protons on the amidinium group and the proton of the NH group. This *in vacuo* calculation probably does not reflect the electrostatic forces involved with binding to the strongly electronegative potential found in the minor groove to DNA and homopolymer.

Acknowledgment. We thank Dr. C. Webster Andrews for the Gaussian calculations and the modifications to the MacroModel force field.

References

(1) Barkley, M. D.; Cheatham, S.; Thurston, D. E.; Hurley, L. H. Pyrrolo[1,4]benzodiazepin Antitumor Antibiotics: Evidence for Two Forms of Tomaymycin Bound to DNA *Biochemistry* **1986**, *25*, 3021–3031.

(2) Denny, W. A. Review: DNA-intercalating ligands as anticancer drugs: Prospects for future design. *Anti-cancer Drug Design* **1989**, *4*, 241–263.

(3) Waring, M. Variation of the supercoils in closed circular DNA by binding of antibiotics and drugs: Evidence for molecular models involving intercalation. *J. Mol. Biol.* **1970**, *54*, 247–277.

(4) Braithwaite, A. W.; Baguley, B. C. Existence of an extended series of antitumor compounds which bind to deoxyribonucleic acid by nonintercalative means. *Biochemistry* **1980**, *19*, 1101–1106.

(5) Larsen, T. A.; Goodsell, D. S.; Cascio, D.; Grzeskowiak, K.; Dickerson, R. E. The structure of DAPI bound to DNA. *J. Biomol. Struct. Dyn.* **1989**, *7*, 477–491.

(6) Kopka, M. L.; Yoon, C.; Goodsell, D.; Pjura, P.; Dickerson, R. E. Binding of an Antitumor Drug to DNA: Netropsin and C-G-C-G-A-A-T-T-^{Br}C-G-C-G. *J. Mol. Biol.* **1985**, *183*, 553–563.

(7) Brown, D. G.; Sanderson, M. R.; Skelly, J. V.; Jenkins, T. C.; Brown, T.; Garman, E.; Stuart, D. I.; Neidle, S. Crystal structure of a berenil–dodecanucleotide complex: The role of water in sequence specific ligand binding. *EMBO J.* **1990**, *9*, 1329–1354.

(8) Pjura, P. E.; Grzeskowiak, K.; Dickerson, R. E. Binding of Hoechst 33258 to the minor groove of B-DNA. *J. Mol. Biol.* **1987**, *197*, 257–263.

(9) Edwards, K. J.; Jenkins, T. C.; Neidle, S. Crystal Structure of a Pentamidine–Oligonucleotide Complex: Implications for DNA-Binding Properties. *Biochemistry* **1992**, *31*, 7104–7109.

(10) Patel, D. J. Netropsin·dG-dG-dA-dA-dT-dT-dC-dC complex: Antibiotic binding at Adenine·Thymine base pairs in the minor groove of the self-complementary octanucleotide duplex. *Eur. J. Biochem.* **1979**, *99*, 369–378.

(11) Cory, M.; Tidwell, R. R.; Fairley, T. A. Structure and DNA Binding Activity of Analogues of 1,5-Bis(4-amidinophenoxy)Pentane (Pentamidine) *J. Med. Chem.* **1992**, *35*, 431–438.

(12) Goodsell, D.; Dickerson, R. E. Isohelical Analysis of DNA Groove Binding Drugs. *J. Med. Chem.* **1986**, *29*, 727–733.

(13) Presented as DNA, Homopolymer Binding and Base Pair Specificity of Minor Groove Binding Bisamidinobenzimidazoles and Bisamidinoindoles by T. A. Fairly, M. Cory, R. R. Tidwell, and I. O. Donkor at the American Chemical Society National Meeting, April 1991, Atlanta, GA. (Abstract MED198).

(14) Kopka, M. L.; Yoon, C.; Goodsell, D.; Pjura, P.; Dickerson, R. E. The molecular origin of DNA-drug specificity in netropsin and distamycin. *Proc. Natl. Acad. Sci. U.S.A.* **1985**, *82*, 1376–1380.

(15) Pullman, B.; Pullman, A. Structural Factors involved in the binding of netropsin and distamycin A to nucleic acids. *Stud. Biophys.* **1981**, *86*, 95–102.

(16) Lee, M.; Krowicki, K.; Hartley, J. A.; Pon, R. T.; Lown, J. W. Molecular Recognition between Oligopeptides and Nucleic Acids: Influence of van der Waals contacts in Determining the 3′-Terminus of DNA sequences Read by Monocationic Lexitropsins. *J. Am. Chem. Soc.* **1988**, *110*, 3641–3649.

(17) Zimmer, C.; Luck, G.; Thrum, H.; Pitra, C.; Binding of analogues of the antibiotics distamycin A and netropsin to native DNA: Effect of the chromophore systems and basic residues of the oligopeptides on thermal stability, conformation and template activity of the DNA complexes. *Eur. J. Biochem.* **1972**, *26*, 81–89.

(18) Bell, C. A.; Cory, M.; Fairley, T. A.; Hall, J. E.; Tidwell, R. R. Structure-activity relationships of pentamidine analogs against *Giardia lamblia* and correlation of antigiardial activity with DNA-binding affinity. *Antimicrob. Agents Chemother.* **1991**, *35*, 1099–1107.

(19) Bell, C. A.; Hall, J. E.; Kyle, D. E.; Grogl, M.; Ohemeng, K. A.; Allen, M. A.; Tidwell, R. R. Structure-activity relationships of analogs of pentamidine against *Plasmodium falciparum* and *Leishmania mexicana amazonensis*. *Antimicrob. Agents Chemother.* **1990**, *34*, 1381–1386.

(20) Cory, M. Molecular modeling of DNA minor groove binding molecules. *Med. Chem. Res.* **1992**, *1*, 417–424.

(21) Tidwell, R. R.; Geratz, J. D.; Dubovi, E. J. Aromatic amidines: Comparison of their ability to block respiratory syncytial virus induced cell fusion and to inhibit plasmin, urokinase, thrombin, and trypsin. *J. Med. Chem.* **1983**, *28*, 294–298.

(22) Tidwell, R. R.; Geratz, J. D.; Dann, O.; Volz, G.; Zeh, D.; Loewe, H. Diarylamidine derivatives with one or both of the aryl moieties consisting of an indole or indole-like ring. Inhibitors of arginine-specific esteroproteases. *J. Med. Chem.* **1978**, *21*, 613–623.

(23) Copeland, R. A. B.; Day, A. R. The preparation and reactions of 2-benzimidazole carboxylic acid and 2-benzimidazolacetic acid. *J. Am. Chem. Soc.* **1943**, *65*, 1072–1075.

(24) Cohen, G.; Eisenberg, H. Viscosity and Sedimentation Study of Sonicated DNA–Proflavine Complexes. *Biopolymers* **1969**, *8*, 45–55.

(25) Roberts, T. D.; Munchausen, L.; Shechter, H. Ortho neighboring-group participation of amides in photolytic hydration of triple bonds. *J. Am. Chem. Soc.* **1975**, *97*, 3112–3117.

(26) Cory, M.; McKee, D. D.; Kagan, J.; Henry, D. W.; Miller, J. A. Design, Synthesis, and DNA Binding Properties of Bifunctional Intercalators. Comparison of Polymethylene and Diphenyl Ether Chains Connecting Phenanthridine. *J. Am. Chem. Soc.* **1985**, *107*, 2528–2536.

(27) Mohamadi, F.; Richards, N. G. J.; Guida, W. C.; Liskamp, R.; Lipton, M.; Caufield, C., Chang, G.; Hendrickson, T.; Still, W. C. Macro-Model-An Integrated Software System for Modeling Organic and Bioorganic Molecules using Molecular Mechanics. *J. Comput. Chem.* **1990**, *11*, 440–467.

(28) Frisch, M. J.; Head-Gordon, M.; Schlegel, H. B.; Raghavachari, K.; Binkley, J. S.; Gonzales, C.; Defrees, D. J.; Fox, D. J.; Whiteside, R. A.; Seeger, R.; Melius, C. F.; Baker, J.; Martin, R.; Kahn, L. R.; Stewart, J. J. P.; Fluder, E. M.; Topiol, S.; Pople, J. A.; Gaussian Inc., Pittsburgh, PA, 1988.

(29) Singh, U. C.; Kollman, P.; Gaussian 80 UCSF. *QCPE Bull.* **1982**, *2*, 117–118.